TU Delft

Delft University of Technology

# An investigation on the circumferential surface crack growth in steel pipes subjected to fatigue bending

Li, Zongchen; Jiang, Xiaoli; Hopman, Hans; Zhu, Ling; Liu, Zhiping

**DOI**
10.1016/j.tafmec.2019.102403

**Publication date**
2020

**Document Version**
Final published version

**Published in**
Theoretical and Applied Fracture Mechanics

**Citation (APA)**
Li, Z., Jiang, X., Hopman, H., Zhu, L., & Liu, Z. (2020). An investigation on the circumferential surface crack growth in steel pipes subjected to fatigue bending. *Theoretical and Applied Fracture Mechanics*, *105*, Article 102403. https://doi.org/10.1016/j.tafmec.2019.102403

**Important note**
To cite this publication, please use the final published version (if applicable).
Please check the document version above.

**Copyright**
Other than for strictly personal use, it is not permitted to download, forward or distribute the text or part of it, without the consent of the author(s) and/or copyright holder(s), unless the work is under an open content license such as Creative Commons.

**Takedown policy**
Please contact us and provide details if you believe this document breaches copyrights.
We will remove access to the work immediately and investigate your claim.

*This work is downloaded from Delft University of Technology.*
*For technical reasons the number of authors shown on this cover page is limited to a maximum of 10.*

Theoretical and Applied Fracture Mechanics 105 (2020) 102403

Contents lists available at ScienceDirect

Theoretical and Applied Fracture Mechanics

journal homepage: www.elsevier.com/locate/tafmec

# An investigation on the circumferential surface crack growth in steel pipes subjected to fatigue bending

Zongchen Li[a,*], Xiaoli Jiang[a], Hans Hopman[a], Ling Zhu[b], Zhiping Liu[c]

[a] Department of Maritime and Transport Technology, Delft University of Technology, 2628 CD Delft, the Netherlands
[b] Departments of Naval Architecture, Ocean and Structural Engineering, School of Transportation, Wuhan University of Technology, 430063 Wuhan, PR China
[c] Laboratory of Intelligent Manufacture and Control, Wuhan University of Technology, 430063 Wuhan, PR China

ARTICLE INFO

*Keywords:*
Steel pipes
Circumferential surface crack
Surface crack growth rate
Analytical method
Structural integrity

ABSTRACT

In the present paper, we propose an analytical method to calculate the Stress Intensity Factor (SIF) of circumferential surface cracks in steel pipes subjected to bending. In light of pipe geometry and bending load case, the analytical formula is raised by introducing new bending correction factors and new geometry correction factors on the basis of the Newman-Raju's method. The bending correction factors are deduced based on the bending stress gradient, while the geometry correction factors are determined by parametric studies for internal surface cracks and external surface cracks respectively. Owing to a large data set requirement by the parametric studies, three-dimensional finite element (FE) models of evaluating SIFs of circumferential surface cracks are developed. The FE method is validated to ensure that it could provide accurate SIF estimations. Analytical verification is conducted which shows that the SIF evaluated by the proposed analytical method match well with the results evaluated by the recommended analytical method. Then experimental investigations of external surface crack growth in offshore steel pipe subjected to fatigue bending are implemented to further validate the analytical method of predicting surface crack growth rate. The analytical results match well with the test results and the available experimental data from literature, indicating that the analytical method can be used for practical purposes and facilitate the crack growth evaluation and residual fatigue life prediction of cracked steel pipes.

## 1. Introduction

The offshore steel pipe is one of the most widely used pipelines in the offshore oil and gas industry [1]. In marine environment, steel pipes bear dynamic loads long-termly, generated by wave, current, wind, and 2nd order floater motions [1,2]. The cyclic bending load, as a dominant load case, commonly applied on critical zones such as hang-off zone, sag bend, arch bend and the touch down zone [2]. Meanwhile, circumferential surface cracks often appear on the surface of the steel pipes initiate from corrosion pitting or girth weld defects [3–5]. Under this circumstance, surface cracks might continually and circumferentially propagate to through-thickness cracks, which might eventually result in leakage or collapse [6,7].

Rational predicting surface crack growth is crucial to avoid such accidents. Appropriate evaluation method therefore is significant in practical applications. Researchers attempted to understand the mechanism of circumferential surface crack growth in pipe by means of numerical and analytical approaches [8–10]. In general, surface crack growth rate is estimated by the Paris' law [11], and the Stress Intensity Factor (SIF) is the assessment criteria,

$$K_I = \sigma\sqrt{\pi A}\cdot F, \tag{1}$$

which is determined by the nominal stress $\sigma$, the crack length $A$, and the boundary correction factor $F$. In terms of surface cracks in a certain scenario, appropriate influential parameters are needed to be identified in order to give rational SIF evaluations. On this basis, researchers proposed a series of analytical methods [8–10,12–14].

The weight function method considers any individual influential factors by introducing corresponding weight functions. In past a few decades, a series of weight functions were proposed [15–17]. The weight function method for circumferential cracked pipes subjected to bending is [18]

$$K_I = F\cdot\sigma_b\cdot\sqrt{\pi\frac{a}{Q}}, \tag{2}$$

where $\sigma_b$ is the bending stress. The $a$ is the crack depth of the surface

* Corresponding author.
*E-mail address:* z.li-8@tudelft.nl (Z. Li).

https://doi.org/10.1016/j.tafmec.2019.102403
Received 10 July 2019; Received in revised form 31 October 2019; Accepted 31 October 2019
Available online 04 November 2019
0167-8442/ © 2020 The Authors. Published by Elsevier Ltd. This is an open access article under the CC BY license (http://creativecommons.org/licenses/BY/4.0/).

**Nomenclature**

| | |
|---|---|
| $A$ | crack length |
| $a$ | crack depth of surface cracks |
| $a_0$ | notch depth |
| $a/c$ | aspect ratio of surface cracks |
| $b$ | plate width |
| $C$, $m$ | the Paris' law constants |
| $c$ | half crack length of surface cracks |
| $c_0$ | half notch length |
| $D$ | external diameter of pipes |
| $d$ | internal diameter of pipes |
| $da/dN$ | crack growth rate along the depth direction |
| $dc/dN$ | crack growth rate along the length direction |
| $F$ | boundary correction factor |
| $f$ | normalized SIF |
| $f_c$ | geometry correction factor of circumferential surface crack in pipe |
| $f_{ci}$ | geometry correction factor of circumferential internal surface crack in pipe |
| $f_{ce}$ | geometry correction factor of circumferential external surface crack in pipe |
| $f_\varphi$ | the correction factor of the eccentric angle of a surface crack |
| $G$ | bending correction factor by considering stress gradient effect |
| $g$ | correction factor of $a/t$, $a/c$ and $\varphi$ |
| $H$ | bending correction factor for flat plate |
| $L$ | pipe length |
| $L_e$ | external span of the four-point bending test |
| $L_i$ | inner span of the four-point bending test |
| $M$ | bending moment |
| $M_1$, $M_2$, $M_3$ | correction factor for the semi-elliptical shape of the crack |
| $Q$ | approximation factor |
| $t$ | thickness of the pipe |
| $R$ | stress ratio |
| $Ri$ | inner radius of the pipe |
| $\sigma$ | nominal stress |
| $\sigma_t$ | nominal tensile stress |
| $\sigma_b$ | maximum of the bending nominal stress |
| $K_I$ | Mode-I stress intensity factor |
| $K_{I,FE}$ | the SIF calculated by finite element method |
| $\Delta K_{Ia}$ | the range of SIFs of the deepest point |
| $\Delta K_{Ic}$ | the range of SIFs of the surface point |
| $\varphi$ | the eccentric angle of a surface crack |
| $\varphi_c$ | the eccentric angle for the surface point |

crack. $Q$ is an approximation factor [19]. $F$ is the influential coefficients depending on the component geometry and crack dimensions, which is calculated by sixth order polynomials within which the coefficients are determined by discrete values tabulated in a table index. Therefore, it is infeasible to continuously evaluate the SIF during the crack propagation. In addition, the complicated influential coefficients and their computation make it inconvenient for usage.

The Newman-Raju's method, as the benchmark solution for surface cracked plane plate, is a well-recognized alternative [13]. This method is also employed in BS 7910 [20] for circumferential external surface cracks, which identifies $\sigma$ and $F$ by curving fitting and engineering judgement

$$K_I = (\sigma_t + H\sigma_b)\sqrt{\pi\frac{a}{Q}}F\left(\frac{a}{t}, \frac{a}{c}, \frac{c}{b}, \varphi\right), \tag{3}$$

where $\sigma_t$ and $\sigma_b$ represents tension stress and bending stress respectively, $H$ is a correction function for the bending nominal stress, $F(a/t, a/c, c/b, \varphi)$ is the boundary correction factor

$$F = \left[M_1 + M_2\left(\frac{a}{t}\right)^2 + M_3\left(\frac{a}{t}\right)^4\right]f_\varphi g f_w, \tag{4}$$

where $M_1$, $M_2$ and $M_3$ are the correction factor for the semi-elliptical shape of the crack, $f_\varphi$ is the correction factor of the eccentric angle of surface cracks, and $g$ can be regard as a correction factor of crack shape evolving along with crack propagation, $f_w$ is a correction factor for the finite width of a plate geometry. The numerical method is capable to evaluate the SIFs of any stage during the crack growth process. In addition, besides the SIFs of the surface point and deepest point, the SIF of any point along the crack front is able to be evaluated. However, Eq. (3) was originally proposed for flat plates, thus when applying it to cracked pipes, the SIFs are often underestimated [21,22], leading to an overestimate prediction of the residual fatigue life, which might be dangerous for usage.

The aim of this paper is to propose an analytical method to evaluate the SIFs of circumferential surface cracks in steel pipes subjected to bending. Because of a large data set requirement by parametric studies to determine geometry correction factors of the analytical method, in Section 2, three-dimensional finite element (FE) models of evaluating

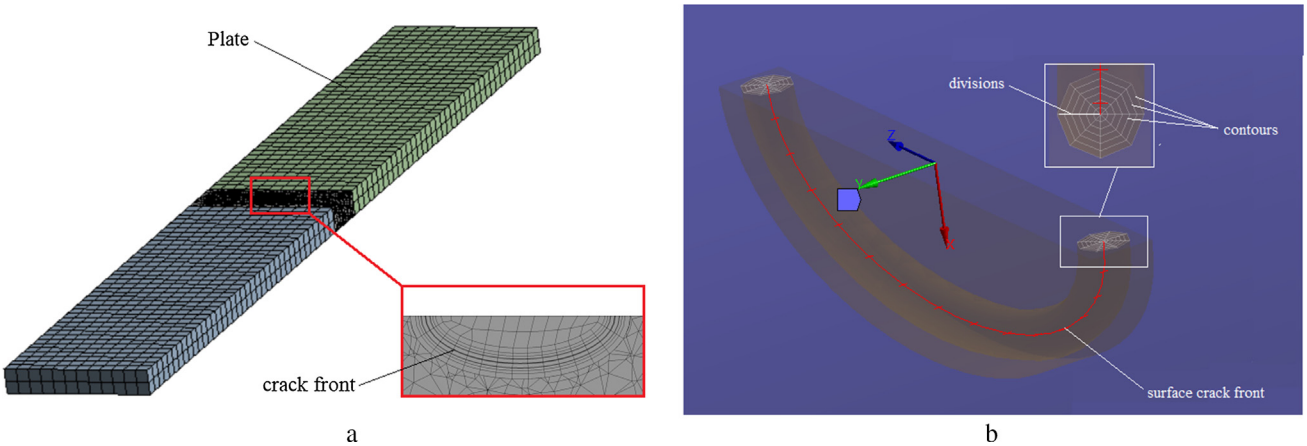


**Fig. 1.** Surface cracked plate model for sensitivity analysis purpose: (a) global meshing condition and local meshing condition around the surface crack; (b) contours around the surface crack front and their divisions.

SIFs of circumferential surface cracks are first developed and validated. In Section 3, the analytical formula is deduced, of which its geometry correction factors are determined by means of FE-based parametric studies. In Section 4, the proposed analytical method of evaluating the SIF is verified by a recommended analytical method. In Section 5, experimental studies of circumferential external surface crack growth in steel pipes subjected to fatigue bending are conducted. Together with available experimental data from literature, the analytical method is validated. Finally the conclusions of this paper are stated in Section 6.

## 2. Three-dimensional finite element analysis

The three-dimensional finite element (FE) method is a reliable method to evaluate SIFs of surface cracks. Rational results can be obtained through proper modelling methods [23]. In order to guarantee the accuracy of SIF evaluation, a sensitivity analysis is first conducted to determine appropriate modelling strategy (e.g., element type, meshing size, modelling contours and divisions around crack tip). Afterwards, using the modelling method, FE models of surface crack in pipe subjected to bending are developed and validated by available experimental data from literature to further ensure their feasibility for pipe scenario.

### 2.1. Surface crack modelling

The FE analysis is conducted using the commercial code ANSYS. Surface cracks are created through the Semi-elliptical Crack module in ANSYS workbench 19 [24]. In order to determine appropriate surface crack modelling strategy, a sensitivity analysis is carried out on a surfaced crack plate, as indicated in Fig. 1. In order to generate ordered elements around the crack front, six contours which are concentric circles centred on the crack front with a number of divisions are modelled, as shown in Fig. 1b. The plate is modelled using 20 nodes three-dimensional solid element 'solid186', whose size is 400 mm long, 60 mm wide and 10 mm thick. One edge face of the plate is fixed supported, while a pure tension is applied on the other edge face. The surface crack is located at the middle of the plate, perpendicular to the tension load. It is semi-elliptical shaped, with crack depth $a = 2.0$ mm, half crack length $c = 4.0$ mm. The plate applies tetrahedral meshing method [25], while the surface crack uses hexahedral dominant meshing method [23]. Then the SIFs along surface cracks are evaluated through the displacement extrapolation method, and compared with the Newman-Raju's analytical method [26], as shown in Figs. 2 and 3.

The comparing results shown in Fig. 2 indicated that the SIF should be obtained at least from the third contour. The mesh sensitivity study shows that the SIFs obtained from the deepest point and the surface point using a tetrahedron meshing method has a good agreement with the Newman-Raju's method [13], whereas the mesh size of the elements around the surface crack does not significantly influence the SIFs, as shown in Fig. 3. In this paper, to ensure a robust and accurate evaluation, a 2.0 mm element size is adopted for the areas around the surface crack, and the mesh size around the surface crack front are controlled by the number of contour and their divisions (see in Fig. 1b); while for the other area a 5.0 mm element size is used. The division numbers of each contour from 8 to 20 is studied as well, which has a negligible influence to the SIF evaluation; therefore, eight divisions of each contour are chosen.

### 2.2. The FE analysis of surface cracked steel pipes subjected to bending

Since the surface crack modelling strategy have been determined, the modelling method is applied to the FE analysis of circumferential surface cracked steel pipes subjected to bending. As illustrated in Fig. 4a of the 4-point bending scenario, the pipe is positioned horizontally, supported by two support units. A pair of vertical loads are applied on the load units, generating a bending moment $M$ onto the pipe. Therefore, the nominal bending stress $\sigma_b$ can be calculated as

$$\sigma_b = \frac{M}{\frac{\pi \cdot D^3}{32} \cdot \left(1 - \frac{d}{D}^4\right)} \tag{5}$$

where $\sigma_b$ is the maximum bending nominal stress, $D$ and $d$ are the external and internal diameter of the pipes respectively. The surface crack is circumferentially located in the middle of the tension side of the pipe model, either in the internal surface or the external surface, propagating in the cross-section plane, as shown in Fig. 4b. The details and shape parameters of the surface crack is shown in Fig. 4c. Fig. 5 shows the steel pipe model and the meshing conditions. The steel pipe is created by three merged parts for different meshing purposes: required by the crack modelling method, the middle part where the surface crack is located uses tetrahedral meshing method; while the other two parts are meshed using sweep meshing method. Hexahedral dominant meshing method is adopted for the surface crack.

In order to ensure the accuracy of the pipe models, the FE method is further validated by available experimental data from literature, i.e., three sets of internal surface cracked pipes subjected to bending [21] and two sets of external surface cracked pipe subjected to bending [22]. Table 1 listed the five test specimens, along with the 4-point bending

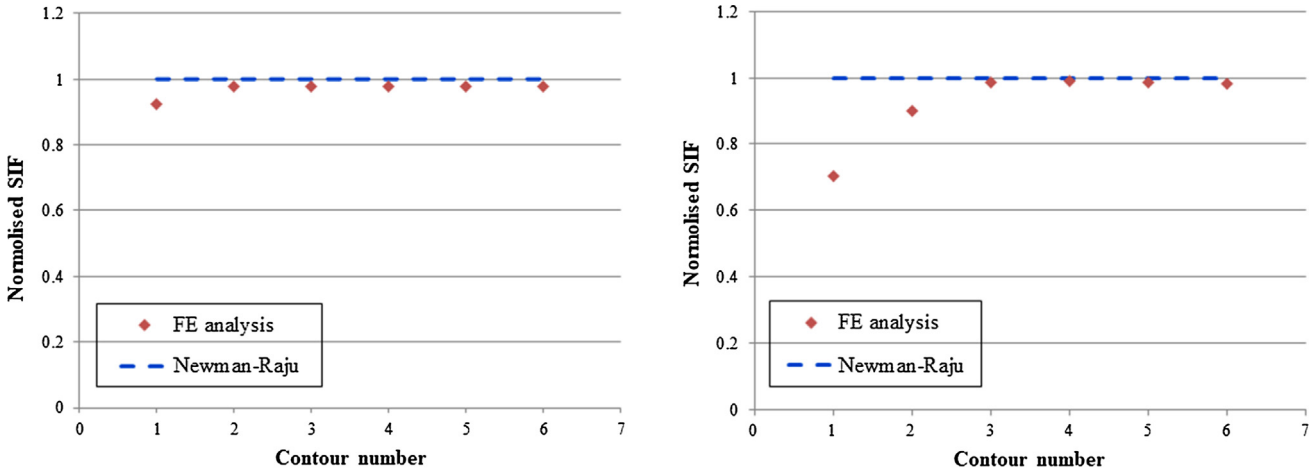


**Fig. 2.** Sensitivity study of contour numbers.

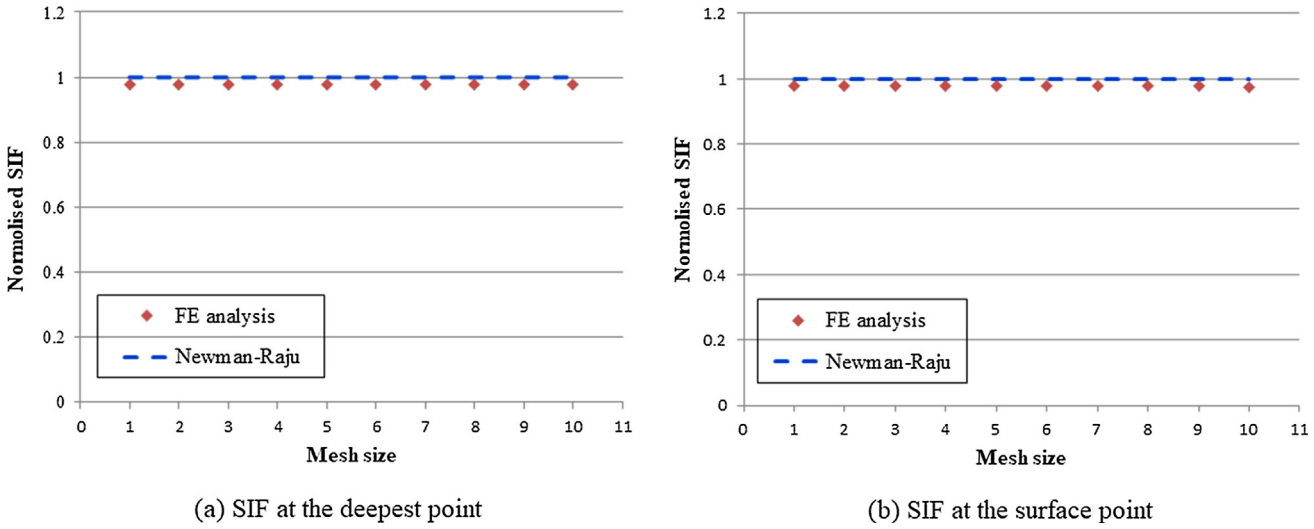


**Fig. 3.** Sensitivity study of element size of the elements around the surface crack.

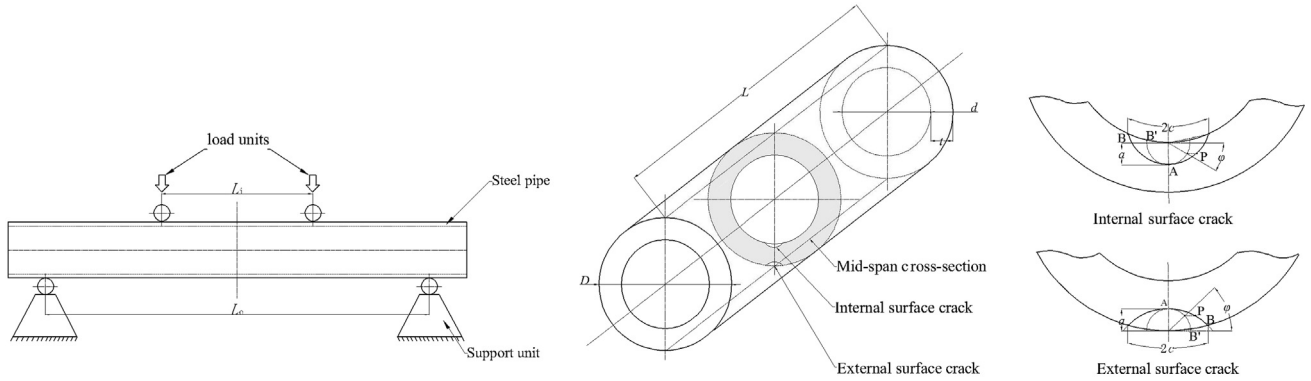


**Fig. 4.** (a) Schematic diagram of a surface cracked steel pipe subjected to 4-point bending; (b) the location of the internal and external surface crack; (c) the dimensions of the internal and external surface crack.

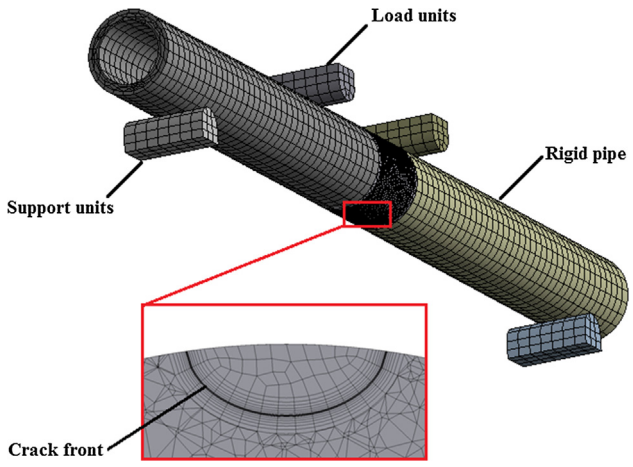


**Fig. 5.** Global mesh condition of the FE model and the local meshing around the surface crack.

setup, material properties, size of the pipes, initial crack sizes, and load condition. Then the five FE models are built in the light the corresponding specimen sizes, crack dimensions and load condition. Afterwards, the SIFs of surface cracked steel pipes subjected to bending are calculated. Then, incorporate with Paris law which is

$$da/dN = C(\Delta K_{Ia})^m, \quad (6)$$

$$dc/dN = C(\Delta K_{Ic})^m, \quad (7)$$

the crack growth rate along the length direction and depth direction are estimated respectively. In Eqs. (6) and (7), $da/dN$ and $dc/dN$ are the crack growth rate along the depth direction and along the length direction respectively, $\Delta K_{Ia}$ and $\Delta K_{Ia}$ are the range of stress intensity factors of the deepest point and the surface point respectively, $C$ and $m$ are two material constants which keep consistent with the referenced value, as listed in Table 2. Afterwards, by assuming a small amount of cycles, the increments of the crack length and depth are calculated. Eventually, it is possible to trace the surface crack growth along the two directions. The detailed procedure of evaluating surface crack growth is indicated in Fig. 6.

The global stress distribution of FE model 'FI-2' and the local stress distribution around the internal surface crack on the internal surface is shown in Fig. 7. Fig. 7a shows that the stress concentrates in the mid-bottom of the pipe where the surface crack is located. More detailed, the local stress distributed around the surface crack as a butterfly shape is shown in Fig. 7b. Under the bending moment, the surface crack opening is observed (displayed as eleven times than the true scale).

Fig. 8 shows the comparison of $a/c$ versus $a/t$ between the FE results and the available experimental data of internal surface cracked steel pipes. The FE results match well with the available experimental data from literature, which implies that the FE method is appropriate to

**Table 1**
Detail information of FE models.

| Model index | Crack location | 4-point bending set-up | | Material properties | | Notch and pipe size (mm) | | | | Load condition (KN) | |
|---|---|---|---|---|---|---|---|---|---|---|---|
| | | $L_i$ (mm) | $L_e$ (mm) | $\sigma_y$(MPa) | $\sigma_u$(MPa) | $c$ | $a$ | $D$ | $t$ | Max | Min |
| FI-1 [21] | Internal surface | 245 | 1000 | 227 | 406 | 22.75 | 4.5 | 102 | 8.1 | 27.54 | 2.75 |
| FI-2 [21] | Internal surface | 245 | 1000 | 227 | 406 | 5.0 | 5.0 | 102 | 8.1 | 44.76 | 4.48 |
| FI-3 [21] | Internal surface | 245 | 1000 | 227 | 406 | 18.25 | 3.0 | 102 | 8.1 | 27.54 | 2.75 |
| FE-1 [22] | External surface | 600 | 1260 | 318 | 650 | 18.0 | 4.3 | 168 | 14.8 | 185.0 | 18.5 |
| FE-2 [22] | External surface | 600 | 4300 | 450 | 593 | 61.5 | 12.4 | 324 | 28.5 | 460.0 | 50.0 |

*$L_i$ and $L_e$: internal and external span of the 4-point bending, $\sigma_y$: yield strength, $\sigma_u$: ultimate strength, $c$: half crack length, $a$: crack depth, $D$: external diameter of pipes, $t$: pipe wall thickness.

**Table 2**
The Paris constants for each specimen.

| Model index | Paris constant | |
|---|---|---|
| | $C$ | $m$ |
| FI-1 [21] | $3.2 \times 10^{-10}$ | 3.72 |
| FI-2 [21] | $3.2 \times 10^{-10}$ | 3.72 |
| FI-3 [21] | $3.2 \times 10^{-10}$ | 3.72 |
| FE-1 [22] | $1.917 \times 10^{-12}$ | 3.195 |
| FE-2 [22] | $2.29 \times 10^{-14}$ | 4.4 |

*The Paris constant employed in crack growth calculations (in all cases examined, units for $da/dN$ and $dc/dN$ are mm/cycle, and the SIF in MPa/$m^{1/2}$, respectively).

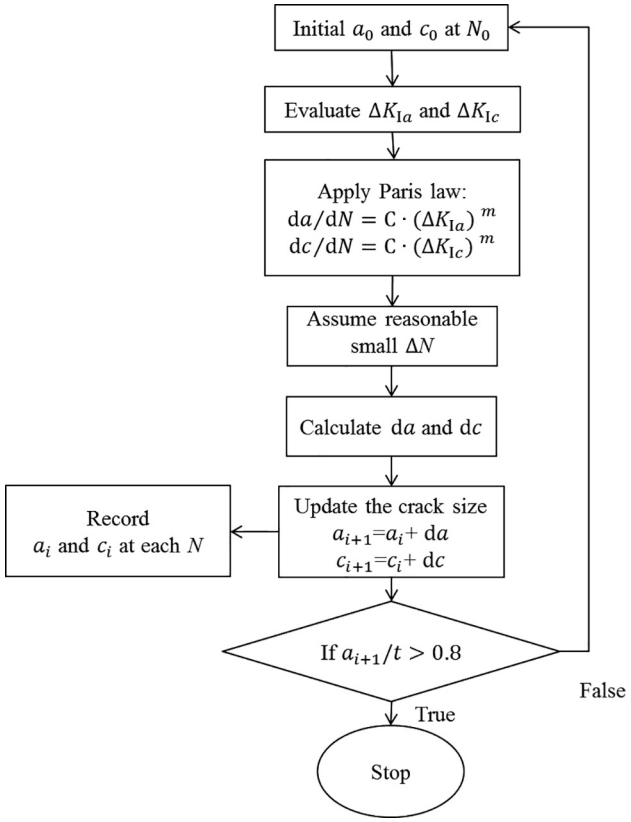


**Fig. 6.** The procedure of evaluating surface crack growth.

evaluate the SIF of internal surface cracks. The comparisons of external surface crack growth results between the FE method and available experimental data are shown in Fig. 9. The FE analysis gives accurate predictions of crack growth along both the depth direction and the length direction. In summary, the validations indicate that the FE analysis is suitable to evaluate the SIFs of circumferential external surface cracks in pipes subjected to bending. Note that external load cases examined here are characterized by stress ratio equal to $R = 0.1$. Then a parametric study on the basis of the FE method therefore will be implemented to determine the geometry correction factor of the analytical method in Section 3.

## 3. The analytical method of evaluating the SIFs of circumferential surface cracked steel pipes subjected to bending

Although the FE method is a reliable method, its high requirement of user expertise and time-consuming restrict its application, particularly for practical situations. The analytical method is a high-efficiency and user friendly method. In this section, an analytical method is proposed based on the Newman-Raju's method [13]. The influence of curved pipe shape is considered by deducing bending correction factors and reassessing the geometry correction factors.

### 3.1. The bending correction factor

The bending correction factor $H$ in Eq. (3) is developed for plate, which is inappropriate for pipe scenario. Here we introduce the new bending correction factor $G$ by considering the stress gradient of pipe subjected bending, as shown in Fig. 10; thus the analytical formula can be expressed as

$$K_I = G \cdot \sigma_b \cdot \sqrt{\pi \frac{a}{Q}} \cdot F. \tag{8}$$

Because the nominal stress distribution adjacent to a point "P" along the surface crack front varies in terms of its location, the bending correction factor $G$ for modifying the stress distribution adjacent to 'P' therefore can be calculated as:

(i) for internal surface crack

$$G = \frac{2a \cdot \sin\varphi + d}{D}, \tag{9}$$

(ii) for external surface crack

$$G = \frac{D - 2a \cdot \sin\varphi}{D}, \tag{10}$$

where $\varphi$ is the eccentric angle of a surface crack, as shown in Fig. 10. The eccentric angle of the deepest point equals to $\pi/2$, while the eccentric angle of the surface point $\varphi_c$ is calculate as

$$\varphi_c = \frac{\pi}{2} - \frac{\pi - \frac{c}{D/2}}{2} = \frac{c}{D}. \tag{11}$$

Different from the plate geometry which the eccentric angle of the surface point equals to 0, $\varphi_c < 0$ for internal surface cracks while $\varphi_c > 0$ for external surface cracks, because of the curved pipe surface.

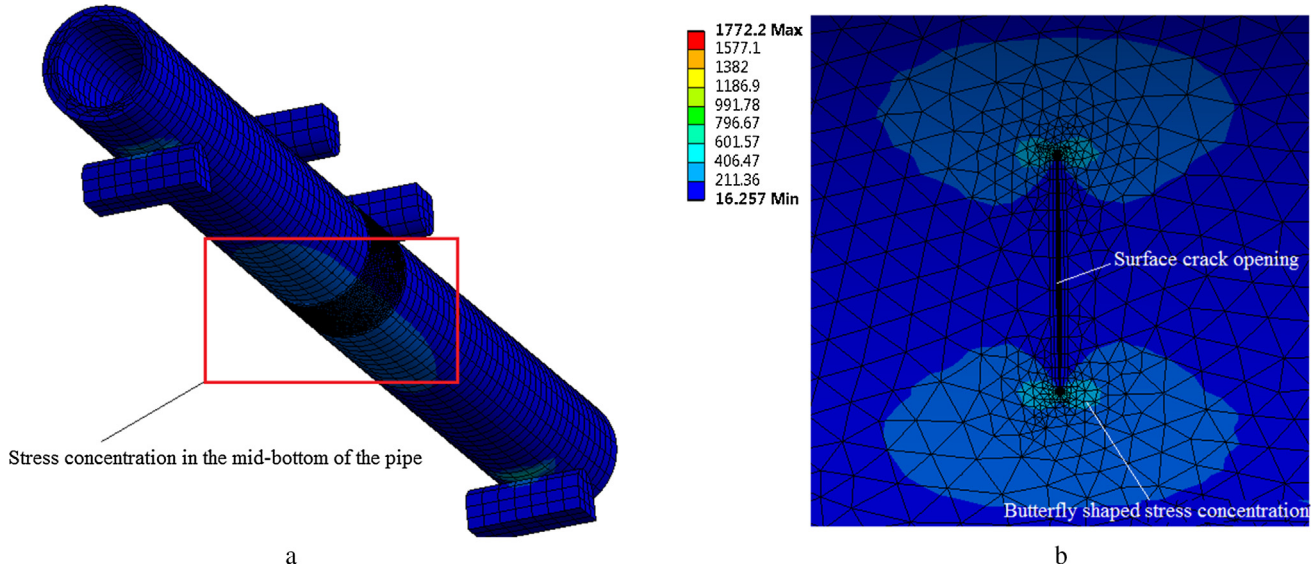


**Fig. 7.** (a) global stress distribution of FE model 'FI-2'; b) local stress distribution around the internal surface crack.

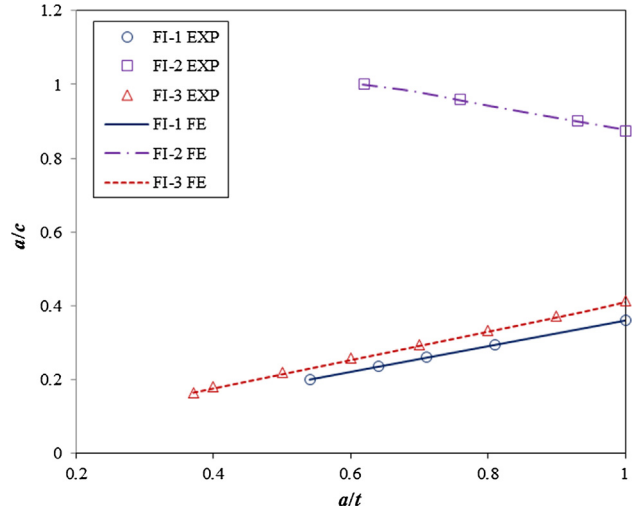


**Fig. 8.** The comparison of $a/c$ versus $a/t$ between FE results and available experimental data of internal surface cracks [21].

### 3.2. The parametric study to determine the geometry correction factor

The boundary correction factor of Eq. (4) is not developed for bending pipe scenario, further improvements are needed. In Eq. (4), $M_1$, $M_2$ and $M_3$ are the correction factor for the semi-elliptical shape of the crack, $f_\varphi$ is the correction factor of the eccentric angle of surface cracks, and $g$ can be regarded as a correction factor of crack shape evolving along with crack propagation. These coefficients aim to correct the SIFs because of the semi-elliptical shape of surface cracks. However, unlike plates, pipes are closed and curved structures; the $f_w$ to correct the finite width of plates is inappropriate for pipes. Therefore, we introduce $f_c$ as the geometry correction factor for circumferential surface cracked pipe subjected to bending. The boundary correction factor is then expressed as

$$F = \left[M_1 + M_2\left(\frac{a}{t}\right)^2 + M_3\left(\frac{a}{t}\right)^4\right] f_\varphi g f_c, \tag{12}$$

where the coefficients except $f_c$ are keep constant with those in Eq. (4), which can be calculated referring to Ref. [13].

In order to determine a rational evaluation method of $f_c$, a FE-based parametric study is conducted. A series of FE models, which are the permutation and combination of nine sets of $t/D$ ranging from 0.04 to 0.20 with the interval of 0.02, 19 sets of $a/c$ with the range of [0.2, 1.0] and interval of 0.1, and seven sets of $a/t$ of [0.2, 0.8] with the interval of 0.1, are built for internal and external surface cracked pipes respectively. Due to the FE modelling capability, the range of $c/d$ is limited to (0, 0.8].

The $K_I/f_c$ results, which represent the SIF evaluations without considering $f_c$ using Eq. (8), are analyzed before the determination of $f_c$. The results indicate the semi-elliptical crack shape correction factors, i.e., $M_1$, $M_2$, $M_3$, $f_\varnothing$, and $g$, provide an rational estimation of the SIFs

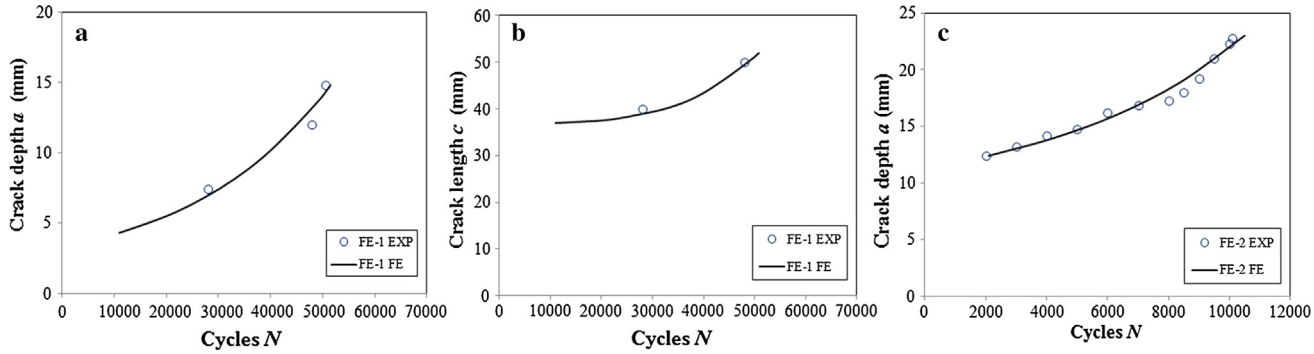


**Fig. 9.** The comparison between the available experimental data and the FE results (FE-1 FE, and FE-2 FE): (a) crack growth along the depth direction of FE-1; (b) crack growth along length direction of FE-1; (c) crack growth along depth direction of FE-2.

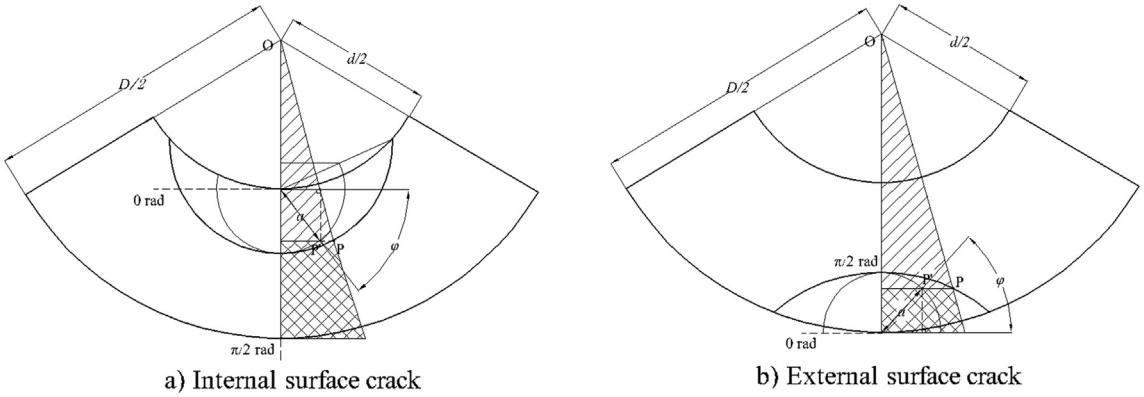


**Fig. 10.** Stress gradient effect on bending nominal distribution around the surface cracks.

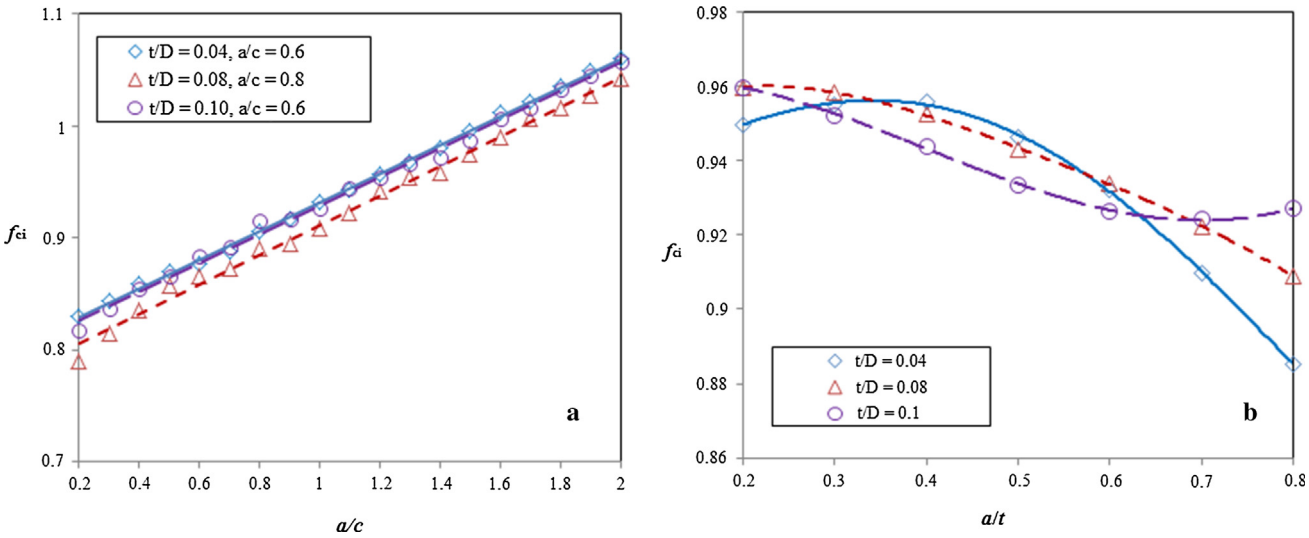


**Fig. 11.** Examples of curve-fitting method of internal surface cracks: (a) $f_{ci}^{1}$ as a function of $t/D$ and $a/c$, (b) $f_{ci}^{2}$ as a function of $a/t$ when $a/c$ = 1.0.

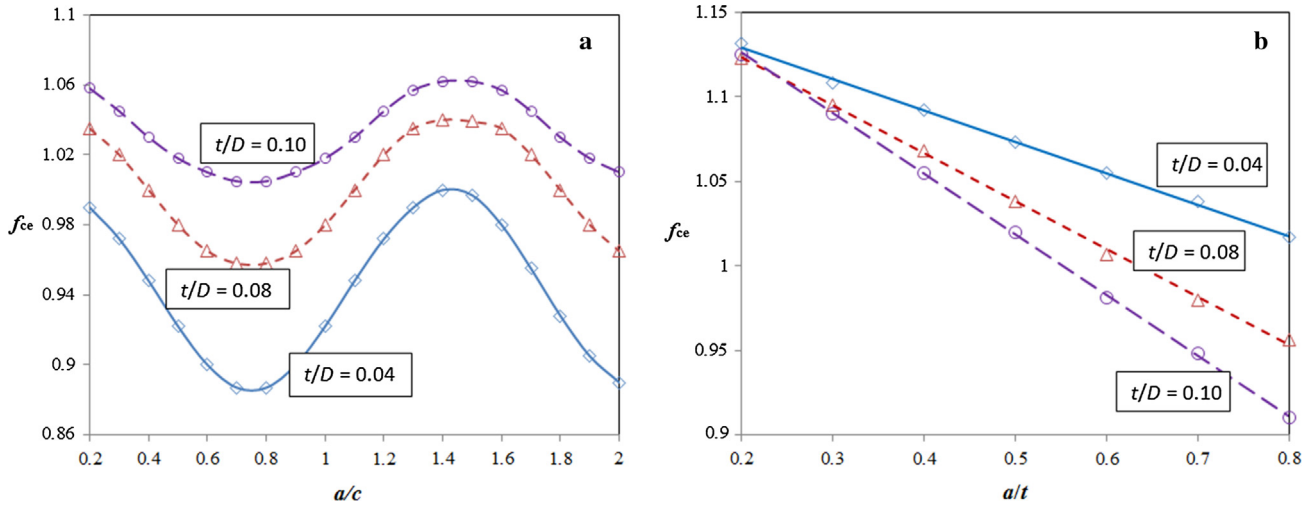


**Fig. 12.** Examples of curve-fitting method of external surface cracks: (a) $f_{ce}^{1}$ as a function of $t/D$ and $a/c$, (b) $f_{ce}^{2}$ as a function of $t/D$ and $a/t$.

distribution trend along the crack front, while the SIFs are overall deviated to the SIFs estimated by FE method. We therefore choose the deepest point of surface cracks to determine $f_c$. Then the SIFs of the deepest point of each model are calculated through the FE method, represented as $K_{I,FE}$. Then $f_c$ can be calculated through

$$f_c = \frac{K_{I,FE}}{G\cdot\sigma_b\cdot\sqrt{\pi\frac{a}{Q}}\cdot\left[M_1 + M_2\left(\frac{a}{t}\right)^2 + M_3\left(\frac{a}{t}\right)^4\right]\cdot f_\varnothing\cdot g}. \tag{13}$$

From Fig. 10, we noticed that the crack shape is influenced by the curved pipe surface, which might affect the value of $f_c$. In addition, the $f_c$ for the crack on the external or internal surface also might be

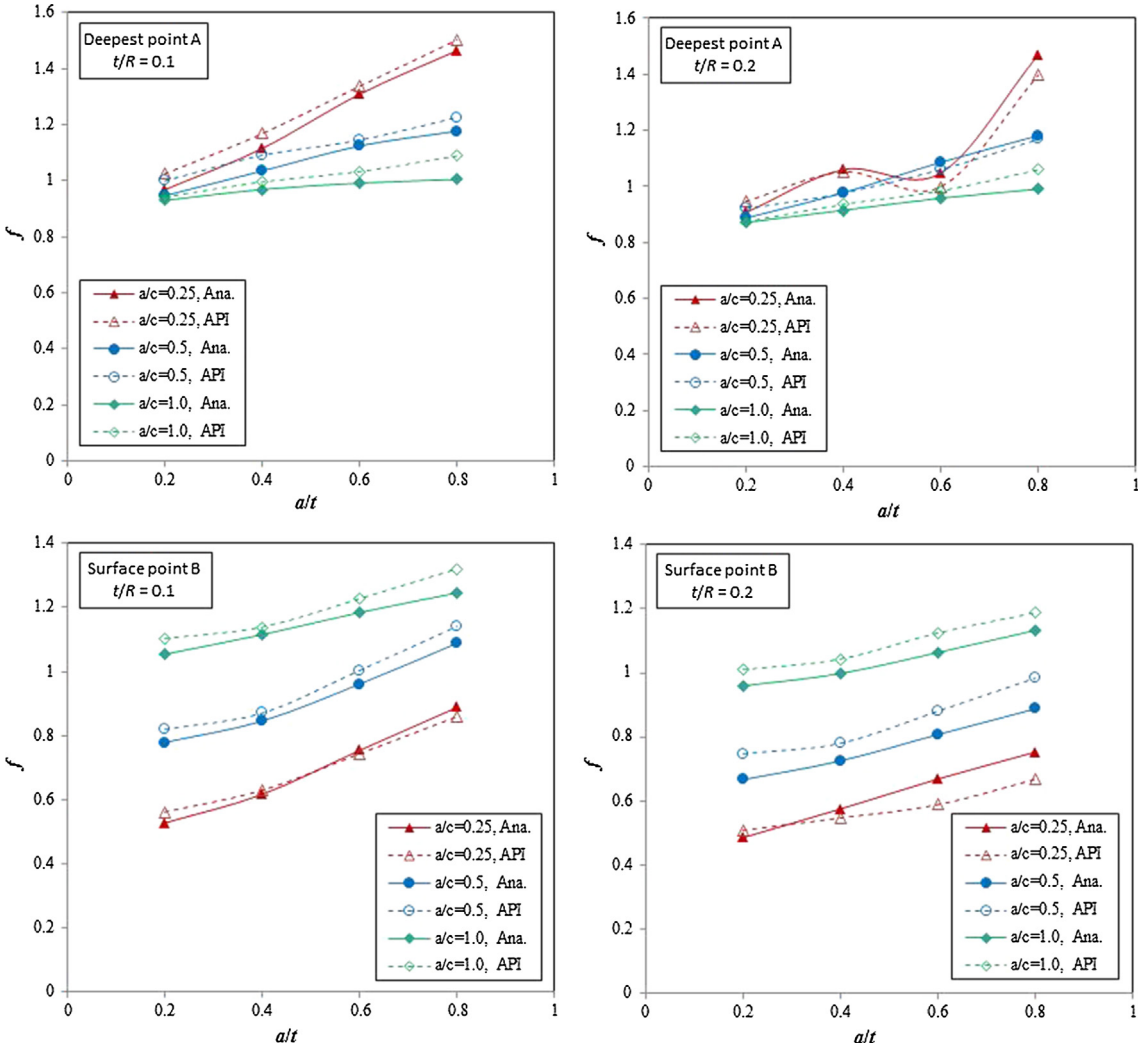


**Fig. 13.** The comparison of the normalized SIF $f$ of internal surface crack between the proposed analytical method and the API 579-1/ASME FFS-1 recommended analytical method [18].

different. Therefore, the $f_c$ for the internal and external surface cracks are determined respectively by the parametric study, defined as $f_{ci}$ and $f_{ce}$ correspondingly.

When obtaining the values of $f_c$ with their corresponding $t/D$, $a/c$ and $a/t$ ratios through Eq. (13), their inherent relationship is analyzed, in order to proposed an analytical equation of $f_{ci} = f(t/D, a/c, a/t)$. By analysing all the data, it is found that the $a/c$ ratio is an independent influential factor (shown in Fig. 11a), where $f_{ci}$ and $a/c$ can be fitted as a linear equation with the similar gradient and y-intercept of all cases with different $t/D$ and $a/t$ ratio. Therefore $f_{ci}$ can be expressed as $f_{ci} = f_{ci}^1(a/c)\cdot f_{ci}^2(a/t, t/D)$, where $f_{ci}^1(a/c)$ is

$$f_{ci}^1\left(\frac{a}{c}\right) = 0.081\cdot\frac{a}{c} + 0.88. \tag{14}$$

Afterwards, the relationship between $f_{ci}^2(a/t, t/D)$ and the other two influential factors $t/D$ and $a/t$ is further investigated. It can be observed from Fig. 11b that $f_{ci}^2$ has a non-linear relationship with the value of $a/t$ and $t/D$. It should be noted that higher order polynomials might be appropriate to curve-fit $f_c$, which is not adopted in this paper. For the purpose of simplify calculation, we use a sinusoidal equation to curve-fit the $f_{ci}^2(a/t, t/D)$. In addition, by analyzing the calculated results, it is found that the periodicity and the phase position are influenced by $t/D$. The $f_{ci}^2$ therefore can be expressed as

$$f_{ci}^2 = \sin\left(\omega\frac{a}{t} + \varphi\right) \tag{15}$$

Once the value of $f_{ci}^1$ of different $a/c$ has been determined, the relation between$f_{ci}^2$ and the $a/t$ with different $t/D$ values are obtained. Afterwards, through curve-fitting method, the corresponding values of $\omega$ and $\varphi$ with different $t/D$ ranging from 0.04 to 0.20 are calculated. The curve-fitting results show that both $\omega$ and $\varphi$ have an approximately linear relation with the variation of $t/D$ ratio, which are fit as

$$\omega = -8.36\cdot\frac{t}{D} + 1.15, \tag{16}$$

$$\varphi = 5.3325\cdot\frac{t}{D} + 1.09, \tag{17}$$

thus

$$f_{ci} = \sin\left(\omega\frac{a}{t} + \varphi\right)\cdot\left(0.081\cdot\frac{a}{c} + 0.88\right), \tag{18}$$

with its $R$-square value equals to 0.948.

The $f_{ce}$ is identified by the same method of $f_{ci}$. By data analysis, it is observed that the $f_{ce}$ presents a sinusoidal variation trend with the variation of $a/c$ ratio, while the $t/D$ ratio influences the amplitude value and the intercept value, as indicated in Fig. 11a. In addition, $f_{ce}$ has a linear relationship with $a/t$ ratio, of which the slope value is determined by the $t/D$ ratio, as shown in Fig. 12b. Therefore $f_{ce}$ can be expressed as

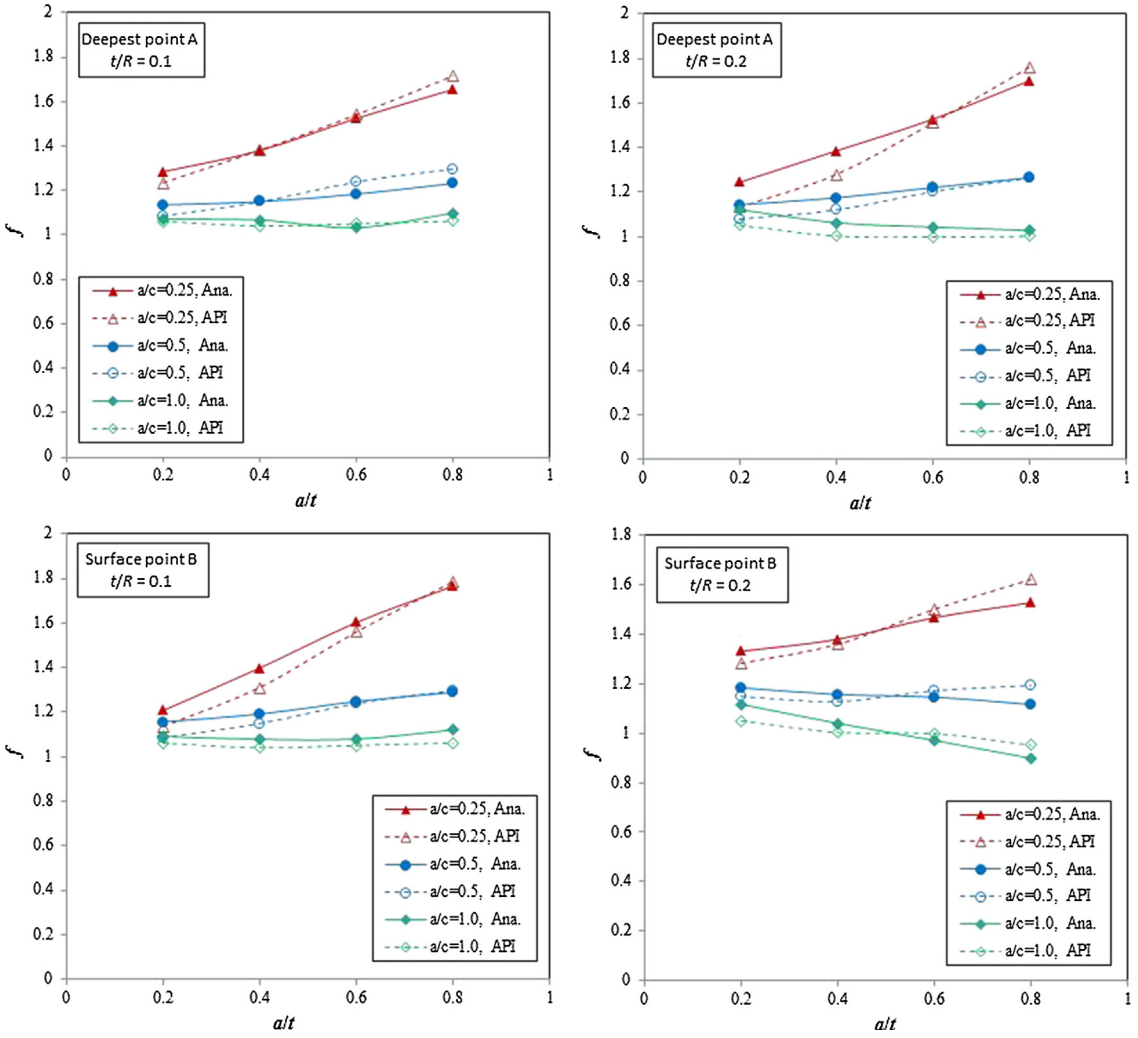


**Fig. 14.** The comparison of the normalized SIF $f$ of external surface crack between the proposed analytical method and the API 579-1/ASME FFS-1 recommended analytical method [18].

**Table 3**
Pipe specimen category and details.

| Specimen | $L$ (mm) | $D$ (mm) | $t$ (mm) | $a$ (mm) | $c$ (mm) |
|---|---|---|---|---|---|
| PE-1-1 | 2000 | 168.3 | 12.76 | 2.31 | 4.94 |
| PE-1-2 | 2000 | 168.3 | 12.81 | 2.48 | 5.04 |
| PE-1-3 | 2000 | 168.3 | 12.77 | 2.44 | 4.89 |
| PE-2-1 | 2000 | 168.3 | 12.70 | 2.39 | 3.99 |
| PE-2-2 | 2000 | 168.3 | 12.74 | 2.44 | 3.82 |
| PE-2-3 | 2000 | 168.3 | 12.68 | 2.39 | 3.99 |
| PE-3-1 | 2000 | 168.3 | 12.61 | 3.99 | 4.00 |
| PE-3-2 | 2000 | 168.3 | 12.73 | 3.96 | 3.98 |
| PE-3-3 | 2000 | 168.3 | 12.84 | 3.92 | 3.97 |

*The parameters, i.e., $D$, $t$, $a$, $c$, are measured from each specimens, each of which is the weighted average of three measurement locations.

$f_{ce} = f^1_{ce}(a/c,\ t/D)\cdot f^2_{ce}(a/t,\ t/D)$, where $f^1_{ci}(a/t)$ is

$$f^1_{ce}\left(\frac{a}{c}\right) = n\cdot\sin\left(4.6\cdot\frac{a}{c} - 5\right) + k \tag{19}$$

Through curve fitting, we found that the value of $f^1_{ce}$ is influence by $t/D$ as an approximately sinusoidal relation (see in Fig. 12a), where its periodicity and the phase position are influenced by $t/D$. Thus through curve fitting method, the '$n$' and '$k$' is fit as

$$n = -0.04\cdot\frac{t}{D} + 0.072, \tag{20}$$

$$k = 1.5\cdot\frac{t}{D} + 0.8815, \tag{21}$$

Similarly, $f^2_{ce}$ is influenced by $t/D$ as a linear relation (see in Fig. 12b),

$$f^2_{ce}\left(\frac{a}{c}\right) = p\cdot\frac{a}{t} + q \tag{22}$$

thus '$p$' and '$q$' is fit by curve fitting method as

$$p = -2.705\cdot\frac{t}{D} - 0.083, \tag{23}$$

$$q = 0.45\cdot\frac{t}{D} + 1.15. \tag{24}$$

therefore

$$f_{ce} = \left[n\cdot\sin\left(4.6\cdot\frac{a}{c} - 5\right) + k\right]\left(p\cdot\frac{a}{t} + q\right), \tag{25}$$

which has a $R$-square value larger than 0.99.

Therefore, the geometry correction factor $f_c$ can be used in Eq. (12) as the boundary correction factor of the proposed analytical formula of Eq. (8) to evaluate the SIFs of circumferential surface cracks in steel pipes subjected to bending. The analytical formula covers a wide range of pipe geometry and surface crack shapes of $0.2 \le a/t \le 0.8$, $0.2 \le a/c \le 1.0$, $0.04 \le t/D \le 0.20$, $c/d \le 0.8$, which can meet most of the conditions of offshore steel pipes in practical situations.

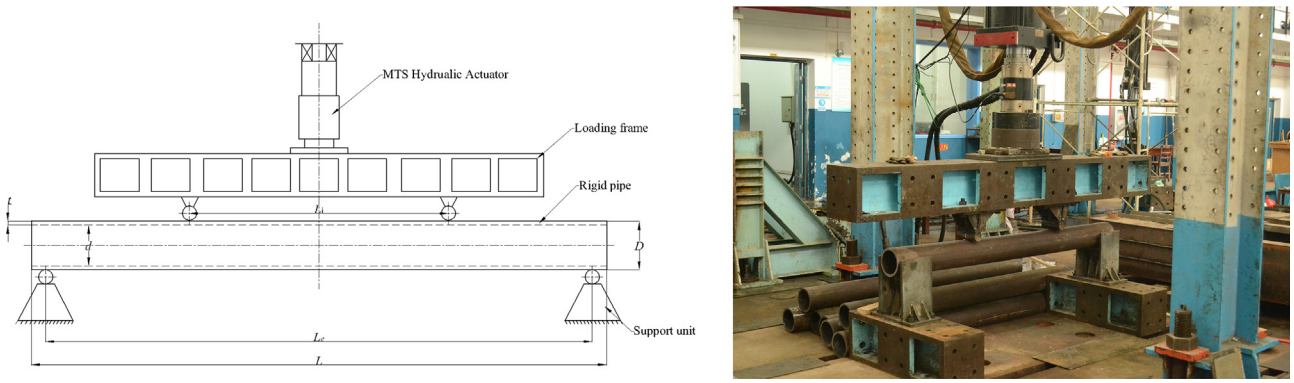


**Fig. 15.** Four-point bending test set-up: the schematic and specimen configuration is shown in left; actual test set-up is shown in right.

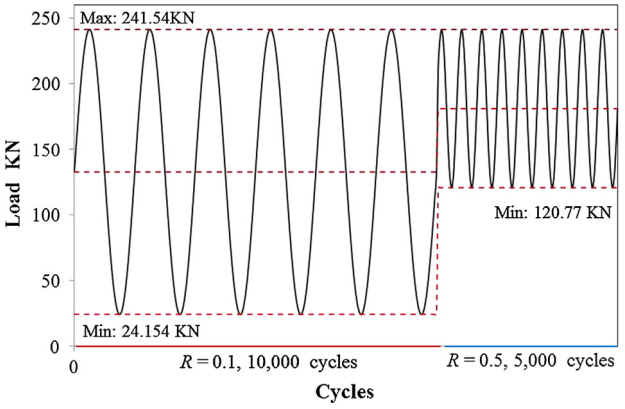


**Fig. 16.** The load spectrum and beach mark generating procedure.

## 4. Verification of the SIF evaluation of circumferential surface cracks in steel pipes subjected to bending

In this section, the SIF evaluation by means of the proposed analytical method is compared with the weight function method, i.e., Eq. (2), recommended by API 579-1/ASME FFS-1 [18]. The boundary correction factor $F$ evaluated by weight function is calculated by

$$F = A_0 + A_1 \cdot \beta + A_2 \cdot \beta^2 + A_3 \cdot \beta^3 + A_4 \cdot \beta^4 + A_5 \cdot \beta^5 + A_6 \cdot \beta^6, \quad (26)$$

where the value of $A_0$ to $A_6$ are referred to the corresponding table sorted by the value of $t/R_i$, $a/c$, and $a/t$. $\beta$ is given as

$$\beta = 2\varphi/\pi \quad (27)$$

here, the range of $\varphi$ is defined as $[0, \pi]$. Therefore, the eccentric angle $\varphi$ for the surface point in Eq. (2) is defined as zero.

In this section, considering the limited tabulated values of $t/R_i$, $a/c$, and $a/t$ provided by Ref. [18], as well as the common surface crack profiles and pipe dimensions (e.g., in most cases, thick-wall pipes are applied) in offshore steel pipe scenarios, the SIF of both internal and external surface cracks within different profiles and pipe dimensions are calculated by the two analytical methods. The $t/R_i$ ratio of 0.1 and 0.2, $a/c$ ratios of 0.25, 0.5, and 1.0, $a/t$ ranges from 0.2 to 0.8 with the interval of 0.2 are chosen for the verification. Note that other values of $t/R_i$, $a/c$, and $a/t$ are impossible to be calculated by Eq. (2) because the corresponding values of $A_0$ to $A_6$ are not included in reference table. The comparison applied the normalized SIF to better illustrate their difference, which is

$$f = \frac{K_I}{\sigma_b \cdot \sqrt{\pi \frac{a}{Q}}}. \quad (28)$$

Then the results using the proposed analytical method (results marked as 'Ana.') and the API recommended analytical method (results marked as 'API') are compared. Fig. 13 shows the result comparison of internal surface cracks in steel pipes, which indicates that the results evaluated by the proposed analytical method match well with the results calculated by the API recommended method, with an average error of 2.6% for the deepest point, and an average error of 3.8% for the surface point. The result comparison of external surface cracks in steel pipes are shown in Fig. 14, the results evaluated by the proposed analytical method match well with the results from the API recommended method, with an average error of 2.3% for the surface point and an average error of 2.8% for the deepest point.

In summary, the verification by means of the API recommend method indicated that the proposed analytical method managed to accurately evaluate the SIF of the surface crack. In addition, unlike the API recommended method which is only able to calculated the SIF with limited tabulated $t/R_i$, $a/c$, and $a/t$ ratios, the proposed analytical method is able to evaluate the SIF along the surface crack front continually during the surface crack growth process within the range of $0.2 \le a/t \le 0.8$, $0.2 \le a/c \le 1.0$, $0.04 \le t/D \le 0.20$, $c/d \le 0.8$.

## 5. Experimental validation of circumferential surface cracked steel pipes subjected to fatigue bending

Experimental studies are conducted in order to further validate the feasibility of the proposed analytical method in terms of predicting

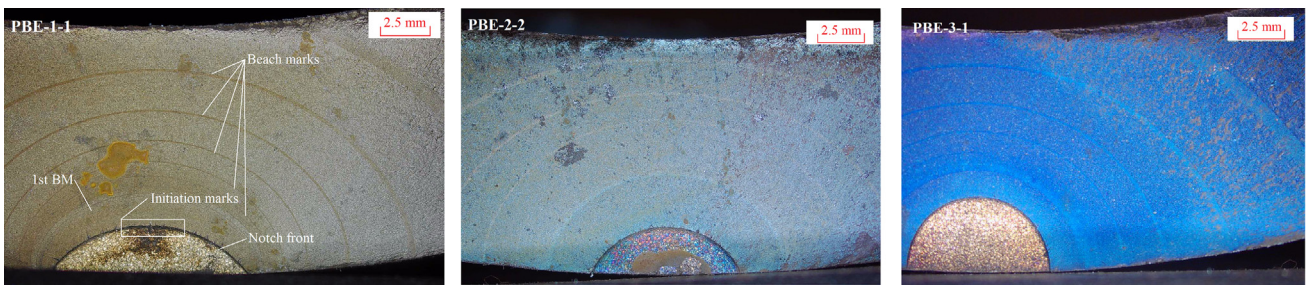


**Fig. 17.** Beach marks on the cross-section of three pipe bending specimens.

**Table 4**
Fatigue test results of circumferential external surface cracked pipes subjected to bending.

| Specimen | PE-1-1 | | PE-1-2 | | PE-1-3 | | PE-2-1 | | PE-2-2 | | PE-2-3 | | PE-3-1 | | PE-3-2 | | PE-3-3 | |
|---|---|---|---|---|---|---|---|---|---|---|---|---|---|---|---|---|---|---|
| Cycles | *a* | *c* | *a* | *c* | *a* | *c* | *a* | *c* | *a* | *c* | *a* | *c* | *a* | *c* | *a* | *c* | *a* | *c* |
| 0 | 3.79 | 5.51 | 6.69 | 7.82 | 4.29 | 5.80 | 5.34 | 6.53 | 5.05 | 6.03 | 6.07 | 6.98 | 5.34 | 5.78 | 5.82 | 6.23 | 5.52 | 5.96 |
| 10,000 | 3.99 | 5.56 | 7.25 | 8.17 | 4.57 | 5.96 | 6.03 | 7.33 | 5.68 | 6.72 | 7.2 | 8.07 | 6.29 | 6.71 | 6.61 | 7.43 | 6.38 | 6.86 |
| 20,000 | 4.36 | 5.77 | 8.48 | 9.64 | 5.14 | 6.29 | 6.98 | 8.24 | 6.58 | 7.79 | 8.79 | 10.51 | 7.45 | 8.01 | 7.72 | 8.92 | 7.48 | 8.43 |
| 30,000 | 4.87 | 6.02 | 10.24 | 12.74 | 6.02 | 7.17 | 8.47 | 10.16 | 7.84 | 9.46 | 10.81 | 14.08 | 8.86 | 10.43 | 9.32 | 11.61 | 8.76 | 10.77 |
| 40,000 | 5.55 | 6.62 | NIL | NIL | 7.15 | 8.71 | 9.77 | 13.38 | 9.27 | 11.93 | NIL | NIL | 10.84 | 13.96 | 11.18 | 15.32 | 10.35 | 14.4 |
| 50,000 | 6.67 | 7.67 | NIL | NIL | 8.720 | 10.91 | 11.86 | 18.46 | 10.86 | 15.76 | NIL | NIL | NIL | NIL | NIL | NIL | NIL | NIL |
| 60,000 | 8.09 | 9.62 | NIL | NIL | 10.80000 | 13.92 | NIL | NIL | NIL | NIL | NIL | NIL | NIL | NIL | NIL | NIL | NIL | NIL |
| 70,000 | 10.11 | 12.01 | NIL | NIL | NIL | NIL | NIL | NIL | NIL | NIL | NIL | NIL | NIL | NIL | NIL | NIL | NIL | NIL |

*All units of *a* and *c* are in mm.

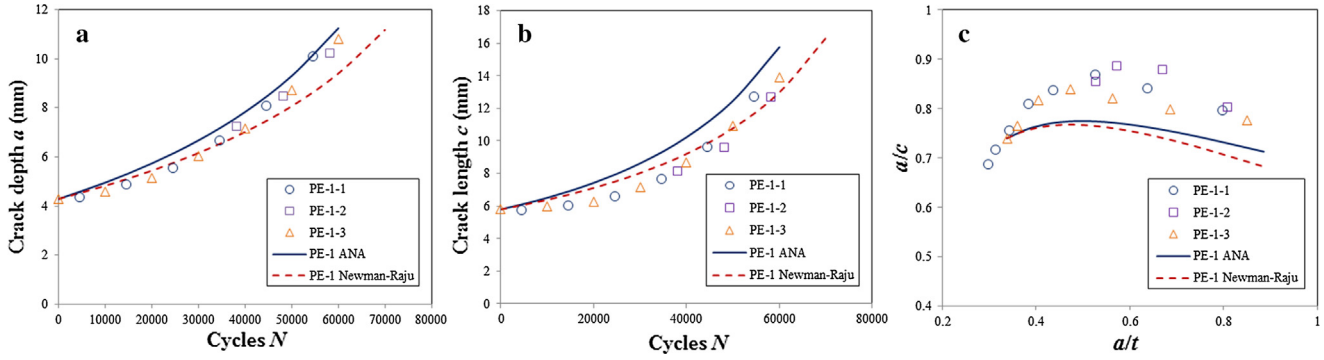


**Fig. 18.** The results comparison of PE-1: (a) crack growth along depth direction; (b) crack growth along length direction; (c) crack aspect ratio variation.

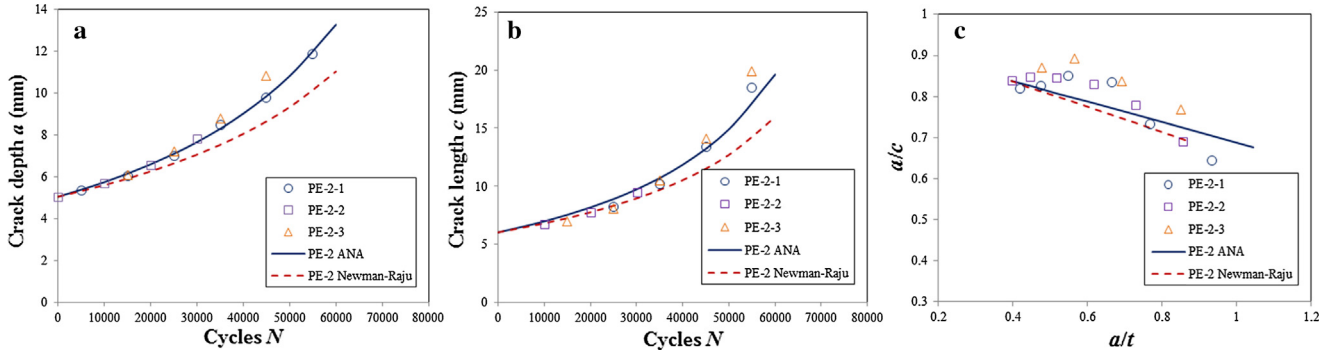


**Fig. 19.** The results comparison of PE-2: (a) crack growth along depth direction; (b) crack growth along length direction; (c) crack aspect ratio variation.

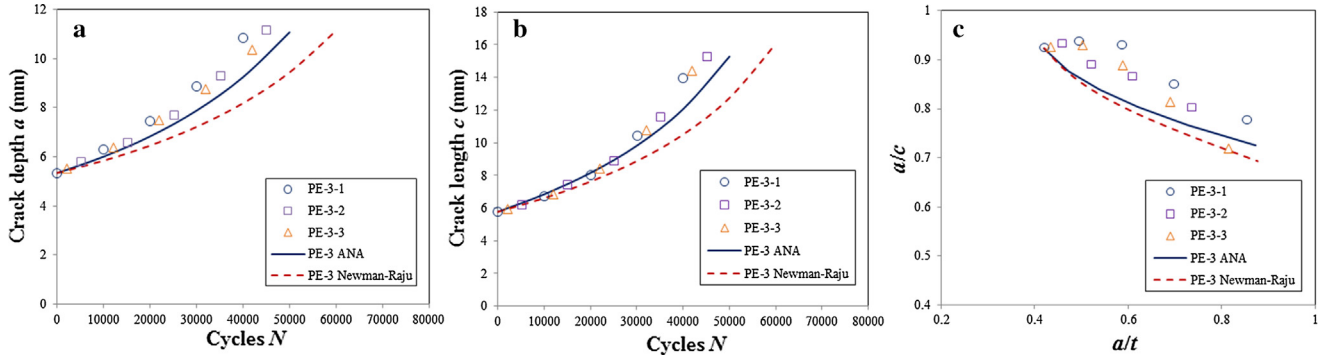


**Fig. 20.** The results comparison of PE-3: (a) crack growth along depth direction; (b) crack growth along length direction; (c) aspect ratio variation.

surface crack growth rate. The experimental results of crack growth rate of external surface cracks in steel pipes subjected to bending are obtained. At the meanwhile, the analytical formula for internal surface crack in steel pipes subjected to bending is validated through available experimental data from literature [21]. It should be noted that three data sets different from those used for validation of FE method are utilized herein to validate the analytical method.

**Table 5**
Detailed information related to geometries, loading and material parameters for the specimens with internal surface crack.

| Specimen | Initial geometry parameters (mm) | | | | Load condition (KN) | | Material constant | |
|---|---|---|---|---|---|---|---|---|
| | *c* | *a* | *D* | *t* | Max | Min | *C* | *m* |
| PI-1 | 6.0 | 3.0 | 102 | 8.1 | 28.92 | 2.89 | $3.2 \times 10^{-10}$ | 3.72 |
| PI-2 | 6.0 | 6.0 | 102 | 12.7 | 30.30 | 3.03 | $3.2 \times 10^{-10}$ | 3.72 |
| PI-3 | 6.0 | 3.0 | 102 | 12.7 | 35.95 | 3.60 | $3.2 \times 10^{-10}$ | 3.72 |

*Unit for d*a*/d*N* and d*c*/d*N* are mm/cycle.

### 5.1. Pipe materials and specimen preparation

Offshore seamless steel pipe API 5L X65, conforming to API code [27], has been used for the experimental study. The pipes have a 168.3 mm external diameter and approximately 12.7 mm thickness. The pipe material has a yield stress of 448 MPa, and tensile stress of 530 MPa, provided by pipe manufacturer.

The detailed parameters of pipe specimens are shown in Table 3. Three types of semi-elliptical notches with different aspect ratio are set up in the pipe specimens. The notches are made by Micro Electric Discharging Machining (Micro-EDM). Each specimen category have three repetitive specimens. For instance, for specimen 'PE-1-1', 'P' means pipe, 'E' represents external surface crack, the first '1' stands for the first type of notch, and the second '1' means the No. of the repetitive specimen.

### 5.2. The full scale pipe bending test

The fatigue tests have been carried out under constant amplitude sinusoidal cyclic loading, generated by MTS Hydraulic Actuator, which has a capacity of 1000 KN. The schematic of test set up is shown in Fig. 15. The load was applied in four-point bending condition to ensure a pure bending statue for the cracked location. In addition, the inner span $L_i$ is designed more than four times larger than the pipe diameter to eliminate possible negative effects from the loading cells, which is 800 mm, while the external span $L_e$ is 1800 mm. Therefore, the bending arm of the test is 500 mm.

Before the fatigue test, a pre-cracking procedure has been conducted to generate fatigue surface cracks initiated from the semi-elliptical notch. This procedure contains two stages of which adopt 80% yield stress and 60% yield stress respectively, as the load amplitude of the constant amplitude sinusoidal cyclic loading. Each stage conducts a certain number of cycles until the surface crack propagate at least 1.0 mm [28]. Then the size of the surface crack after the pre-cracking procedure is regarded as the initial crack size of the surface cracked specimen, which is therefore ready for the fatigue crack growth test.

All the fatigue tests are conducted at room temperature and air environment under load control condition. The loading frequency for pipe bending test is set as 2.5 Hz. The stress ratio *R* maintained 0.1 for the crack growth of all tests. The crack growth process is recorded by beach marking technique by means of changing the stress ratio *R* to 0.5 and cycle for 5000 times, as described in Fig. 16.

### 5.3. Experimental results and validation of the analytical method

After each test, the cross-section of bending specimen has been sampled around the cracked area by oxy-acetylene cutting. Then the beach marks recorded on the cross-section were obtained, as shown in Fig. 17. The crack growth between each adjacent beach marks represents 10,000 cycles; therefore, the cyclic number corresponding to each crack size was recorded, and then measured by an electronic reading microscope. Fig. 17 clearly demonstrates multiple initiations of surface cracks along the notch front, and surface crack continually propagates as a semi-elliptical shape until the crack penetrates the pipe wall. The fatigue tests results are shown in Table 4, all the units of *a* and *c* are in mm.

The test results of crack depth and its corresponding cyclic numbers of the specimens with the same notch size were modified to start from a given starting point, in order to identify the repeatability of the results. Then the surface crack growth of each category was estimated using the procedure shown in Fig. 6: the SIFs of each scenario were calculated by the corresponding proposed analytical method, and the crack growth rate was then estimated using the Paris law. In this part, the material constant *C* is $3.98 \times 10^{-13}$ ($\Delta K$ in MPa/mm$^{1/2}$), and *m* is 2.88, provided by BS 7910 [20] and API 579–1/ASME FFS-1 [18]. Figs. 18–20 shows the comparison of surface crack growth predicted by the analytical method and the test results. In addition, those results were compared with the results evaluated by Newman-Raju's method [13]. It should be noted that the stress ratio for all external loads herein examined is equal to $R = 0.1$.

It is clearly indicated from Figs. 18 to 20 that the experimental results of external surface crack growth in pipes subjected to bending

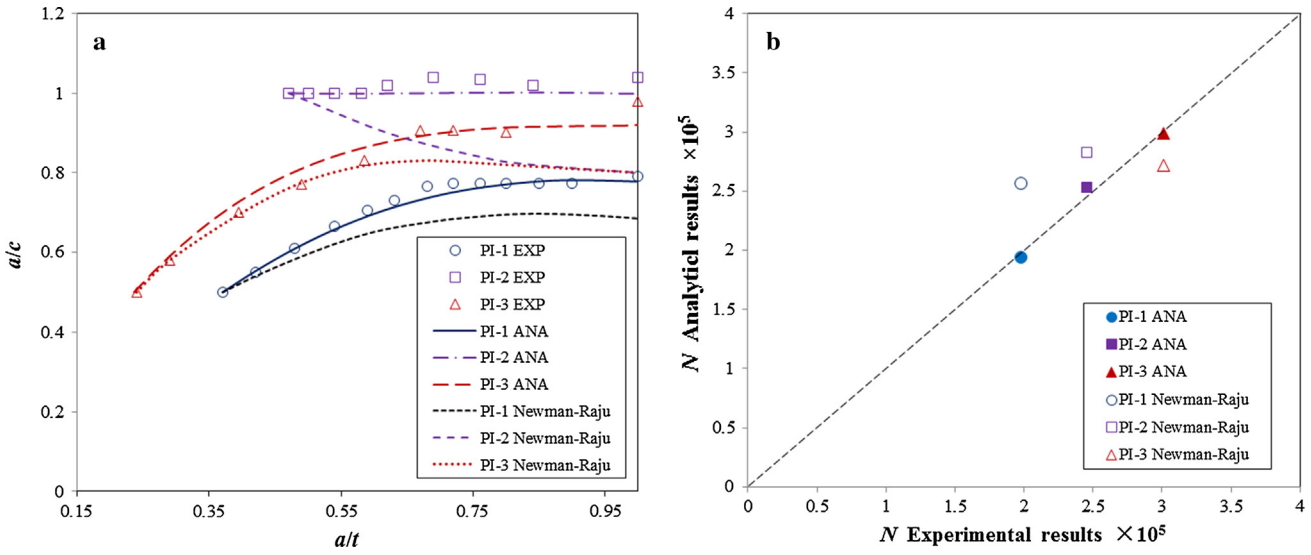


**Fig. 21.** The results comparison of internal surface crack specimens of the experimental results (EXP) [21], the analytical method and Newman-Raju's method: (a) *a*/*c* versus *a*/*t* ratio; (b) fatigue life cyclic numbers.

have a good repeatability. The results estimated by the proposed analytical formula, i.e., PE-1 ANA, PE-2 ANA, and PE-3 ANA, agree well with the experimental results, which perform better than the Newman-Raju's method [13]. In addition, rather than underestimating the crack growth rate, the proposed analytical method stands on the conservative side for the case of PE-1 and PE-2, which might be safer for usage. Similar to the Newman-Raju's method, the $a/c$ versus $a/t$ ratio have been underestimated by the proposed analytical method (see in Figs. 18c, 19c and 20c). The reason might be that the Paris constant $C$ of the surface point and deepest point are different due to a larger plastic zone around the surface point [29]. However, the analytical results agreed better with the experimental data for the $a/c$ versus $a/t$ ratio, owing to the proposed bending correction factor $G$.

The analytical method of estimating the SIFs of internal surface cracks in pipes subjected to bending is validated by three groups of available experimental data from Ref. [21], with different $t/D$ and initial $a/c$ ratio, as given in Table 5. The results of $a/c$ versus $a/t$ ratio are shown in Fig. 21a, which illustrates that the analytical method can predict the variation of the crack profile during the fatigue process more accurately than the Newman-Raju's method. In addition, the fatigue lives of the three specimens predicted by the analytical method, which is the cycles of the crack propagate from the initial size till penetrating the wall, match well with the experimental data, only with an maximum error of 4.79% for PI-2, as shown in Fig. 21b.

## 6. Conclusions

Surface crack growth is a major threat to the structural integrity of offshore steel pipes. Accurately predicting surface crack growth is of great importance to avoid accidents such as leakage and collapse. To date, a series of analytical methods have been developed to estimate the SIFs of surface cracks. However, the influence of the pipe geometry and bending load case have not been fully considered, which often lead to either conservative or non-conservative predictions.

Given that, an analytical method to evaluate the SIFs of circumferential surface cracks in steel pipes subject to bending has been proposed by introducing the bending correction factor $G$, and the geometry correction factor $f_c$. The bending correction is deduced in light of bending stress gradient; while the geometry correction factor is determined by a FE-based parametric study. Owing to a large data set requirement by the parametric studies, three-dimensional finite element (FE) models of evaluating SIFs of circumferential surface cracks are developed and validated.

The proposed analytical method is verified by means of the API recommended analytical method. The SIF results evaluated by the proposed analytical method match well with the results from the recommended analytical method, with an average error of about 2.9%. In addition, the proposed analytical method is not restricted to the limited tabulated $t/R_i$, $a/c$, and $a/t$ ratios, which is capable of continually evaluating the SIF along the surface crack front during the surface crack growth process.

Fatigue experimental investigations have been conducted on external surface cracked API 5L X65 pipes to validate the analytical method for external surface crack growth; while available experimental data were employed to validate the analytical method for internal surface crack growth. The SIF results evaluated by the proposed analytical method matched well with the API recommended analytical method. The prediction of surface crack growth by combing the proposed analytical method and the Paris' law matched well with the experimental results, provided a more accurate prediction than the Newman-Raju's method. The results of $a/c$ versus $a/t$ ratio were underestimated by the analytical method. The reason might be that the Paris constant $C$ of the surface point and the deepest point might be different due to a larger plastic zone around the surface point. In conclusion, the analytical method is appropriate to evaluate the SIF of circumferential surface cracks in steel pipes subjected to bending, which can be utilize for practical purposes to evaluation circumferential surface crack growth and predict residual fatigue life of cracked steel pipes.

## Declaration of Competing Interest

The authors declare that they have no known competing financial interests or personal relationships that could have appeared to influence the work reported in this paper.

## Acknowledgement

The authors appreciate Department of Maritime and Transport Technology, Delft University of Technology, the Netherlands for sponsoring this research. The experimental investigation was supported by Overseas Expertise Introduction Project for Discipline Innovation -111 project of Chinese Ministry of Education and State Administration of Foreign Experts Affair of P. R. China [grant number 444110356] and Department of Maritime and Transport Technology, Delft University of Technology, the Netherlands. The Key Laboratory of High Performance Ship Structure of the Chinese Ministry of Education is also appreciated for providing the experimental facilities. The first author would like to acknowledge the China Scholarship Council, P. R. China [grant number 201606950024] for funding his research.

## References

[1] N.O. Chibueze, C.V. Ossia, J.U. Okoli, On the fatigue of steel catenary risers, Strojniški vestnik-J. Mech. Eng. 62 (2016) 751–756.
[2] S. Kim, M.-H. Kim, Dynamic behaviors of conventional SCR and lazy-wave SCR for FPSOs in deepwater, Ocean Eng. 106 (2015) 396–414.
[3] DNV, Riser Integrity Management. DNVGL-RP-F206, DNV GL, Hovik, Norway, 2008.
[4] DNV, Assessment of Flaws in Pipeline and Riser Girth Welds. DNV-RP-F108, DNV GL, Hovik, Norway, 2017.
[5] R. Brighenti, A. Carpinteri, Surface cracks in fatigued structural components: a review, Fatigue Fract. Eng. Mater. Struct. 36 (2013) 1209–1222.
[6] DNV, Riser Integrity Management, in: DNV Recommended Practice DNVGL-RP-F206, 2008.
[7] DNV, Assessment of flaws in pipeline and riser girth welds, in: DNV Recommended Practice DNV-RP-F108, 2017.
[8] A. Carpinteri, R. Brighenti, A. Spagnoli, Part-through cracks in pipes under cyclic bending, Nucl. Eng. Des. 185 (1998) 1–10.
[9] A. Carpinteri, R. Brighenti, S. Vantadori, Circumferentially notched pipe with an external surface crack under complex loading, Int. J. Mech. Sci. 45 (2003) 1929–1947.
[10] C.D. Wallbrink, D. Peng, R. Jones, Assessment of partly circumferential cracks in pipes, Int. J. Fract. 133 (2005) 167–181.
[11] P. Paris, F. Erdogan, A critical analysis of crack propagation laws, J. Basic Eng. 85 (1963) 528–533.
[12] J. Newman Jr., I. Raju, Analysis of surface cracks in finite plates under tension or bending loads, 1979.
[13] J. Newman Jr, I. Raju, An empirical stress-intensity factor equation for the surface crack, Eng. Fract. Mech. 15 (1981) 185–192.
[14] Y. Peng, C. Wu, Y. Zheng, J. Dong, Improved formula for the stress intensity factor of semi-elliptical surface cracks in welded joints under bending stress, Materials 10 (2017) 166.
[15] E. Folias, On the effect of initial curvature on cracked flat sheets, Int. J. Fract.Mech. 5 (1969) 327–346.
[16] Y. Murakami, L. Keer, Stress intensity factors handbook, vol. 3, J. Appl. Mech. 60 (1993) 1063.
[17] D. Green, J. Knowles, The treatment of residual stress in fracture assessment of pressure vessels, J. Press. Vessel Technol. 116 (1994) 345–352.
[18] A.P.I. API, 579-1/ASME FFS-1: Fitness-for-service, The American Society of Mechanical Engineers, 2016.
[19] A. Russell, Application of Proof Testing to Assess k-Reactor Piping Integrity, Douglas United Nuclear, Inc., Richland, WA (USA), 1970.
[20] B.S.I. BS, Guide on methods for assessing the acceptability of flaws in metallic structures, British Standard Institution, 2015.
[21] Y. Yoo, K. Ando, Circumferential inner fatigue crack growth and penetration behaviour in pipe subjected to a bending moment, Fatigue Fract. Eng. Mater. Struct. 23 (2000) 1–8.
[22] P. Arora, P. Singh, V. Bhasin, K. Vaze, A. Ghosh, D. Pukazhendhi, et al., Predictions for fatigue crack growth life of cracked pipes and pipe welds using RMS SIF approach and experimental validation, Int. J. Press. Vessels Pip. 88 (2011) 384–394.
[23] R. Branco, F.V. Antunes, J.D. Costa, A review on 3D-FE adaptive remeshing techniques for crack growth modelling, Eng. Fract. Mech. 141 (2015) 170–195.

[24] ANSYS, Semi-elliptical Crack. Defines a semi-elliptical crack based on an internally generated mesh to analyze crack fronts by use of geometric parameters. Available: https://ansyshelp.ansys.com/account/secured?returnurl=/Views/Secured/corp/v191/wb_sim/ds_Crack_o_r.html.
[25] H. Okada, H. Kawai, T. Tokuda, Y. Fukui, Fully automated mixed mode crack propagation analyses based on tetrahedral finite element and VCCM (virtual crack closure-integral method), Int. J. Fatigue 50 (2013) 33–39.
[26] J. Newman, I. Raju, Analysis of surface cracks in finite plates under tension or bending loads, 1979.
[27] API, Specification for Line Pipes. API SPEC 5L, American Petroleum Institute, Washington, DC, USA, 2012.
[28] ASTM, ASTM E647. Standard Test Method for Measurement of Fatigue Crack Growth Rates, 1994.
[29] D. Corn, A study of cracking techniques for obtaining partial thickness cracks of pre-selected depths and shapes, Eng. Fract. Mech. 3 (1971) 45–52.